2011 International Workshop on ADC Modelling, Testing and Data Converter Analysis and Design and IEEE 2011 ADC Forum
June 30 - July 1, 2011. Orvieto, Italy.

Using Figures-of-Merit to Evaluate Measured A/D-Converter Performance

Bengt E. Jonsson

ADMS Design AB, Gåsbackavägen 33, SE-820 60 DELSBO, Sweden
phone: +46 70 622 0005
e-mail: bengt.e.jonsson@admsdesign.com

Abstract—This work surveys various figures-of-merit (FOM) that have been used to evaluate and compare measured ADC performance, and takes a first step towards a systematic classification and analysis. Strengths and weaknesses associated with selected figures-of-merit are discussed, and their potential sweet spots or parametric bias is examined using a combination of theoretical analysis and a near-exhaustive set of scientifically reported experimental data. A commonly used FOM is shown to have a distinct, and highly predictable sweet spot with respect to ENOB, and a strong bias towards scaled manufacturing technologies. It is therefore concluded that a continued discussion and treatment of the topic is motivated.

I. Introduction

How do you compare the measured performance of a 5-bit, 1GS/s, flash A/D-converter (ADC) with a Δ-∑ modulator for audio applications in order to determine which of them are "better"? Is it even possible? Although the previous example is extreme, performance benchmarking is increasingly important both for scientific and for commercial ADCs. Within the scientific community there is a need to determine to what extent a recent design advance the state-of-the-art. In order to compare widely different ADCs, various *figures-of-merit* (FOM) have been proposed. A large number of FOM variations may be confusing. On the other hand, if only a small set is widely accepted, the scientific competition will steer towards any bias or sweet spots of such FOM. The strengths and weaknesses of any canonical set of FOM must be properly understood, just as their correlation with theory and the body of empirical results. Of particular interest is how well a particular FOM serves its purpose when it is applied to the measured performance of real circuits. Such analysis must be done statistically, using large amounts of experimental data. The analysis in this work is therefore based on the same data set as the survey in [1], which represents nearly all measured ADC implementations ever published scientifically. Variations of ADC figures-of-merit have often been proposed in the context of presenting a particular circuit implementation – possibly to highlight its particular merits in comparison with prior-art. In this work, the figures-of-merit are put in context of the measured performance of *all* scientific ADCs, with the purpose to highlight the performance of the FOM rather than the ADCs. Due to the vast and complex nature of the topic, it cannot be fully treated within a single paper. The purpose of this paper is to take a first step towards a more systematic treatment of figures-of-merit used to compare measured ADC performance, and to provide tools and a starting point for a continued discussion.

II. Figures-of-merit

To enable a more systematic treatment of the topic, the FOM flora first needs a structured organization. Mathematically, a figure-of-merit F can have almost any shape and form, but nearly all that were proposed to compare ADC performance can be written using the following expression:

$$F = K \times P^{\alpha_P} \times f^{\alpha_f} \times V^{\alpha_V} \times A^{\alpha_A} \times L^{\alpha_L} \times 2^{\alpha_B B} \quad (1)$$

The variables in (1) are generic. Their possible use and interpretation is described in Table I. As an example, f represents a frequency. It would typically be the sampling rate f_s, or the input frequency f_{in}, but it could also be the clock frequency f_{CLK} or any other relevant expression of frequency. The ITRS FOM [2]

Parameter	Type	Typical |*a*|	Examples
K	scaling factor	–	
P	power	0, 1	P_{tot}, $P_{on\text{-}chip}$
f	frequency	0, 1	f_{in}, f_s, BW, ERBW
V	voltage		V_{DD}, V_{FS}
A	area	0, 1	A_{die}, A_{core}
L	length		$L_{min\text{-}CMOS}$
B	number of bits	0, 1, 2	N, ENOB, "SNR-bits", "SFDR-bits"
X_{dB}	performance	0, 1, 2	DR, SNR, SNDR

Table I. Explanation of FOM parameters in (1) and (6).

$$F = \frac{2^{ENOB@DC}\min\left\{f_s, 2\times ERBW\right\}}{P} \tag{2}$$

has $K = 1$, $f = \min\{f_s, 2 \times \text{ERBW}\}$, $B = \text{ENOB @ DC}$, $P = P$, $\alpha_B = 1$, $\alpha_f = 1$, $\alpha_P = -1$, and all other $\alpha = 0$. The most commonly used FOM today,

$$F = \frac{P}{2^{ENOB} f_s} \tag{3}$$

is similar to (2) but differ in that $f = f_s$, $B = \text{ENOB}$, and the entire FOM is inverted so that lower is better. More figures-of-merit found in the literature are listed in Table II, which also show their equivalent *log-form FOM*. The mapping between the linear-form "*F*", and the equivalent log-form "*G*" is based on the mapping of a performance X_{dB} (e.g. SNR) to its equivalent performance in "bits" B, expressed as

$$B = \frac{X_{dB} - 1.76}{6.02} \tag{4}$$

which means that

$$2^{\alpha_B B} = 2^{\alpha_B \frac{X_{dB}-1.76}{6.02}} = \left(10^{\log 2}\right)^{\alpha_B \frac{X_{dB}-1.76}{20\times\log 2}} = 10^{\alpha_B \frac{X_{dB}-1.76}{20}} \tag{5}$$

Thus the base-10 logarithmic equivalent of F in dB can be written as

$$G = X_{dB} + \frac{20}{\alpha_B} \times \left[\alpha_P \log P + \alpha_f \log f + \alpha_V \log V + \alpha_A \log A + \alpha_L \log L\right] + M_0 + M \tag{6}$$

where M is an arbitrary constant, and $M_0 = -1.76$ ($M = 0$) can be used if a strict mapping between F and G is desired. For simplicity, M_0 shall be omitted for the remainder of this paper. The expression for G was made resolution-centric by scaling with $1/\alpha_B$, because most log-form FOM start with a resolution-related parameter such as *dynamic range* (DR), *signal-to-noise-and-distortion ratio* (SNDR), etc., and then add or subtract other terms. An example is the FOM used in [3],

$$G_{B2} = SNDR + 10 \times \log\frac{BW}{P} \tag{7}$$

Inspection of (7) reveals that $B = \text{ENOB}$, $f = \text{BW}$, $\alpha_B = 2$, $\alpha_f = 1$, and $\alpha_P = -1$. Its equivalent linear form is

$$F_{B2} = \frac{2^{2\,ENOB} \times BW}{P} \tag{8}$$

For a FOM where resolution performance is not included ($\alpha_B = 0$), the unscaled version of G (i.e., $20 \times \log \ldots$) can be used. More log form FOM examples are found in Table II. An attempt to group figures-of-merit into classes {A, B, C, … } based on their generic expression is reflected in the ID column of Table II. For lack of better nomenclature, these classes and integer numbers shall be used as in (7) and (8) to refer to specific figures-of-merit for the remainder of this paper.

ID	Linear form (F)	Logarithmic form (G)	Comment
A0	$\frac{P}{2^N \times f_s}$	$SNDR_{ideal} + 20 \times \log \frac{f_s}{P}$	Emmert [4]
A1	$\frac{P}{2^{ENOB} \times f_s}$	$SNDR + 20 \times \log \frac{f_s}{P}$	ISSCC-FOM (common)
A2	$\frac{P}{2^{ENOB@DC} \min\{f_s, 2 \times ERBW\}}$	$SNDR_{DC} + 20 \times \log \frac{\min\{f_s, 2 \times ERBW\}}{P}$	ITRS FOM [2]
A3	$\frac{P}{2^{ENOB} \times 2 \times ERBW}$	$SNDR + 20 \times \log \frac{2 \times ERBW}{P}$	Geelen [5]
A4	$\frac{P}{2^{ENOB} \times f_{in}}$	$SNDR + 20 \times \log \frac{f_{in}}{P}$	Draxelmayr [6]
A5	$\frac{P}{2^{ENOB} \sqrt{2 \times f_{in} \times f_s}}$	$SNDR + 20 \times \log \frac{\sqrt{2 \times f_{in} \times f_s}}{P}$	Jonsson [7]
B1	$\frac{P}{2^{2ENOB} \times f_s}$	$SNDR + 10 \times \log \frac{f_s}{P}$	Thermal FOM [8]
B2	$\frac{P}{2^{2ENOB} \times BW}$	$SNDR + 10 \times \log \frac{BW}{P}$	Devarajan [3]
B3	$K \times \frac{P}{DR^* \times BW}$	$DR_{dB} + 10 \times \log \frac{BW}{P} + M$	Rabii [9] Schreier [10]
C1	$\frac{P \times A}{2^{ENOB} f_s}$	$SNDR + 20 \times \log \frac{f_s}{P \times A}$	Andersen [11]
C2	$\frac{P \times A}{2^{ENOB} \min\{f_s, 2 \times ERBW\}}$	$SNDR + 20 \times \log \frac{\min\{f_s, 2 \times ERBW\}}{P \times A}$	Esperança [12]
C3	$\frac{P \times A}{10^{\frac{DR_{dB} - 1.78}{20}} \times BW}$	$DR_{dB} + 20 \times \log \frac{BW}{P \times A}$	Sauerbrey [13]
D1	$\frac{P \times V_{DD}}{2^{ENOB} \times f_s}$	$SNDR + 20 \times \log \frac{f_s}{P \times V_{DD}}$	Chiu [14]
E1	$\frac{P}{2^{ENOB} \times 2 \times BW \times V_{DD} \times L^2}$	$SNDR + 20 \times \log \frac{2 \times BW \times V_{DD} \times L^2}{P}$	Bechen [15]
F1	$\frac{P}{N \times f_s}$	$20 \times \log \frac{f_s \times N}{P}$	Gambini [16]
G1	$\frac{P}{f_s}$	$20 \times \log \frac{f_s}{P}$	Energy/sample (common)
H1	$\frac{A}{f_s}$	$20 \times \log \frac{f_s}{A}$	Black [17]
I1	$\frac{P}{f_s \times SFDR}$		Merkel [18]
J1	$\frac{P}{2^{\alpha_B \times ENOB} \times f^{\alpha_f} \times V_{DD}^{\alpha_V} \times L^{\alpha_L}}$	$SNDR + M + \frac{20}{\alpha_B} \times [\alpha_f \log f_s + \ldots$ $\ldots + \alpha_V \log V_{DD} + \alpha_L \log L - \log P]$	Vogels [19]

Table II. Examples of FOM found in the literature. Note that all linear-form FOM were written in the "lower-is-better" form to simplify comparison, and all log-form equivalents were sign-inverted for readability.

*) Linear-form DR is assumed to be a power-ratio in this expression.

III. Figures-of-merit at a glance

Table II is not an exhaustive listing of all figures-of-merit ever proposed, but it contains a majority of those that have been proposed in papers where measured performance was reported or analyzed. A quick review of the table reveals some shared and some differentiating features. First of all it is noticed that no FOM except F_{J1} [19] use α-parameters other than $|\alpha| = \{0, 1, 2\}$, and usually $|\alpha| = 1$. The option to curve-fit α-parameters to empirical data as in [19] should be further explored, but is beyond the scope of this paper. It is also seen that the value of α_B defines *the relative weight given to resolution performance* compared to other parameters. This is most obvious in the log-form expressions: Setting $\alpha_B = 2$ scales all other terms with 0.5.

Many FOM proposals are variations on how to define the frequency parameter f in the generic expression (1). This does not necessarily mean that they are unimportant. An appropriate choice of f is essential for a technically sound FOM. Most propose $f = f_s$ or BW (i.e., $f_s/2$), which means that input frequency is completely disregarded. The ability to maintain performance over the entire Nyquist bandwidth has no value in f_s-only figures-of-merit, and this limitation is addressed by some of the other variations: The ITRS FOM F_{A2} [2] use $\text{ENOB}_{@\text{DC}}$ as B, and twice the *effective resolution bandwidth* (ERBW) as f. Clipping is applied so that f does not exceed f_s. ERBW is defined as the input frequency where $\text{ENOB} = \text{ENOB}_{@\text{DC}} - 0.5$. In the author's opinion, this and possibly its unclipped sibling F_{A3}, is one of the best ways to define the frequency parameter f. The only real drawback is that only 10% of all Nyquist ADC papers report ERBW explicitly, although it can be extracted manually from SNDR vs. f_{in} plots, if provided. Input frequency, on the contrary, is reported in most papers. The variation F_{A4}, where f_s is replaced by f_{in}, was proposed in [6]. The obvious drawback with F_{A4} is that the sampling rate performance is discarded instead. Both parameters are important. Combining f_s and f_{in} into a *geometric mean* was proposed by the author in [7], and defines F_{A5}. Scaling f_{in} with a factor of 2 ensures that $F_{A5} = F_{A1}$ at $f_{in} = f_s/2$. At lower input frequencies, F_{A5} downgrades the FOM value, and performance above the first Nyquist band is promoted. A similar permutation could use the *arithmetic mean*, which gives a less severe penalty for reporting only at low f_{in}. The purpose of F_{A5} was to provide a *Nyquist-centric* FOM able to promote designs with performance over the entire Nyquist bandwidth (or more) – much the same way as the ITRS FOM, but that could also handle the lack of ERBW data.

Performance (resolution) is almost exclusively measured in ENOB (SNDR) or dynamic range (DR). The latter is mostly used when comparing Δ-$\sum$ modulators. *Spurious-free dynamic-range* (SFDR) was used in F_{I1}, and nominal resolution N was used in F_{A0}, and F_{F1}. The latter was labeled as a "SAR-friendly FOM" [16], and the energy per sample was divided by N (output word length) rather than 2^N – the motivation being that a SAR ADC more resembles a digital circuit, and thus the power dissipation increase linearly with N. Supply voltage and area awareness was introduced by multiplying with A in the C-class, and V_{DD} in the D-class figures-of-merit. A possible extension would be to have *simultaneous* area and supply-voltage awareness by introducing both A and V at the same time.

IV. FOM properties

While it is beyond the scope of this paper to evaluate the properties of all the listed figures-of-merit, a small selection will be analyzed with respect to their bias and sweet spots. The purpose is to illustrate how a FOM can be evaluated by using a combination of empirical data and theory, and also to give reason for continued discussion and treatment. A significant amount of the scientific competition is currently "FOM-centric". As pointed out by Bult [20], the most intense competition revolves around F_{A1} – also referred to as the "ISSCC" or "Walden" FOM. It will therefore be analyzed and compared to other figures-of-merit.

A. Resolution sensitivity

It was shown in [21] that the state-of-the-art boundary for on-chip energy per sample ($E = P/f_s$) of scientifically published ADCs currently follow a *low-resolution plateau* of **~1 pJ/sample** up to ENOB = 9, after which it follows a thermal noise defined slope approximately described by $\boldsymbol{E = 2^{2(\text{ENOB}-9)}}$ **pJ/sample**. This is shown in Fig. 1 (a). Realizing that F_{A1} and F_{B1} are merely a scaling of E by respectively 2^{ENOB} and $2^{2\text{ENOB}}$, it is expected that the thermal-slope boundary will map to a constant ($\sim 2^{-18}$) for F_{B1}, while the plateau will map to $F_{B1} = 2^{-2\text{ENOB}}$. For F_{A1}, the plateau maps to $F_{A1} = 2^{-\text{ENOB}}$, and the slope to $F_{A1} = 2^{(\text{ENOB}-18)}$. Data and predicted boundaries for F_{A1} and F_{B1} are plotted in Fig. 1 (b) and (c). The plots reveal important properties of the two FOM: By visual inspection of the entire scatter, it is appears that the strong ENOB correlation evident in the energy/sample plot have been balanced out in F_{A1} by the scaling with $2^{-\text{ENOB}}$, while it reappears as a reversed

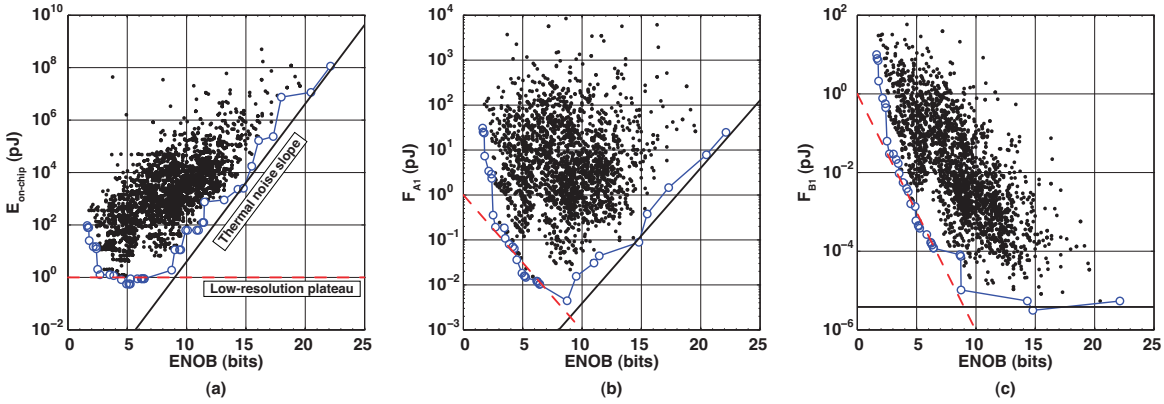

Fig. 1. Plots showing: (a) On-chip energy per sample vs. ENOB, (b) ENOB sweet spot of F_{A1}, and (c) High-resolution bias of F_{B1}. In each successive plot, the data is multiplied by 2^{-ENOB}.

correlation in F_{B1} after one further scaling with 2^{-ENOB}. It can be concluded that F_{B1} has a strong overall *bias towards high-resolution*. Since F_{B1} was proposed as a better representation of high-resolution ADCs [8], this is to be expected. Within the thermal slope region (ENOB ≥ 9), however, the state-of-the-art envelope for F_{B1} is almost flat, except for a slight bias towards the highest resolutions. The weakness of F_{B1} is that it can't be meaningfully used below 9-b ENOB.

The main weakness of F_{A1} is that it has a predictable *sweet spot* around the intersection of the low-resolution energy plateau and the thermal noise slope – currently located around ENOB = 9. This sweet spot is defined by the V-shape formed by the mapping of the thermal noise slope and low-resolution plateau boundaries. It is therefore *inherent to the FOM* as long as these energy/sample limits keep their current slopes. It is assumed that high-resolution ADCs will continue to line up against thermal noise limits in the foreseeable future. The F_{A1} sweet spot will therefore remain, unless the low-resolution energy floor acquires a slope that is 2^{ENOB} or more by pushing the current state-of-the-art envelope stronger at the lowest resolutions. In that case, F_{A1} becomes low-resolution biased instead. While such evolution of low-resolution ADC efficiency might be possible, it is not likely to happen immediately. Since much of the scientific competition has been (and still is) F_{A1}-centric [20], its inherent sweet-spot properties should be understood and discussed by the scientific community. The very existence of a sweet spot is likely to drive many scientific efforts in a particular direction – independent of real-world needs. It should also be noted that F_{A1} and other A-class FOM are (in contrast to F_{B1} and E) **not independent of ENOB anywhere**. This means that F_{A1} can only be used to meaningfully compare ADC power efficiency at a fixed resolution, in which case you might as well use E.

B. Scaling sensitivity

The scaling sensitivity is investigated for F_{A1} and F_{B1} in Fig. 2 (a) and (b). As pointed out in [22], it is seen that F_{A1} improves with every step of process scaling. It thus *promotes the use of new technology* rather than to optimize design within the same node. A similar trend is not seen for F_{B1}. In fact, it has started to *degrade* with

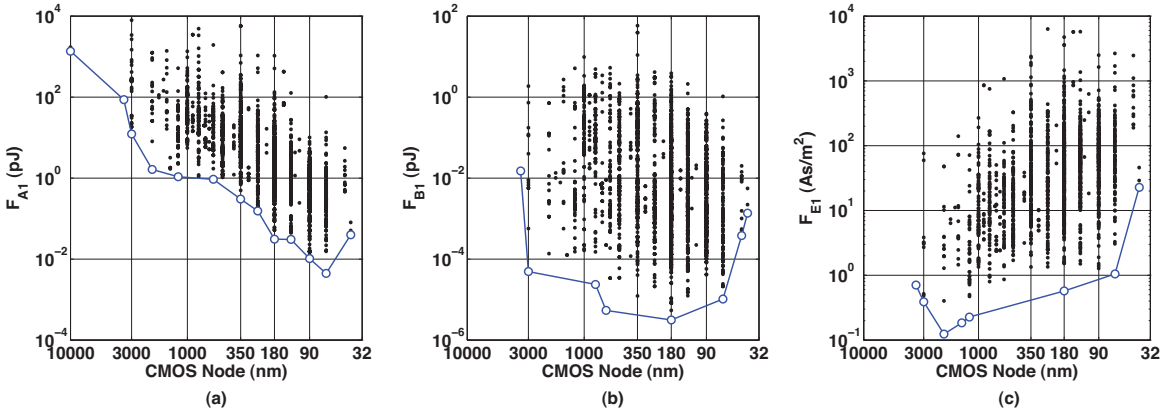

Fig. 2. Plots showing scaling sensitivity of three different FOM: F_{A1}, F_{B1}, and F_{E1}.

scaling, which is further explained in [22]. As another comparison, Bechen proposed F_{E1} as a scaling-independent FOM [15]. As seen from Fig. 2 (c), its state-of-the-art envelope stays within one order of magnitude **from 4 µm to 65 nm** implementations. As a comparison, F_{A1} drops by four orders of magnitude over the same scaling range. This does not necessarily mean that F_{E1}, and F_{B1} are generally "better" than F_{A1}, but it *does* mean that F_{A1} should be annotated with the process node at which the value was achieved, or otherwise used only to compare designs within the same node. This, and the ENOB-sensitivity shown previously, justifies a deeper discussion regarding the proper use of F_{A1} for global ADC performance comparison.

V. Conclusion

Figures-of-merit used in the literature to compare ADC performance were reviewed, and a first step towards a more systematic treatment of the topic was taken. A generic FOM expression was used as a means for classification of FOM types, and the variations within each type were pointed out. A method to analyze properties such as parameter bias or sweet spots was illustrated by applying two commonly used FOM to a near-exhaustive set of scientifically reported ADC performance. It was shown that the most frequently used FOM has a distinct and predictable sweet spot at medium resolutions, and that its state-of-the-art improves with every step of scaling. With a single FOM reaching almost canonical status, it is likely to see a lot of scientific efforts following any bias and sweet spot such FOM might have. It is therefore of great interest both to understand the results shown in this work, and to further investigate and discuss the proper and desired use of figures-of-merit for ADC performance comparison.

References

[1] B. E. Jonsson, "A survey of A/D-converter performance evolution," *Proc. of IEEE Int. Conf. Electronics Circ. Syst. (ICECS)*, Athens, Greece, pp. 768–771, Dec., 2010.
[2] System drivers, International Technology Review for Semiconductors, 2009 Update [Online]. Available: http://www.itrs.net
[3] S. Devarajan, L. Singer, D. Kelly, S. Decker, A. Kamath, and P. Wilkins, "A 16-bit, 125 MS/s, 385 mW, 78.7 dB SNR CMOS pipeline ADC," *IEEE J. Solid-State Circuits*, Vol. 44, pp. 3305–3313, Dec., 2009.
[4] G. Emmert, E. Navratil, F. Parzefall, and P. Rydval, "A versatile bipolar monolithic 6-Bit A/D converter for 100 MHz sample frequency," *IEEE J. Solid-State Circuits*, Vol. SC-15, pp. 1030–1032, Dec., 1980.
[5] G. Geelen, "A 6b 1.1GSample/s CMOS A/D converter," *Proc. of IEEE Solid-State Circ. Conf. (ISSCC), San Francisco*, California, pp. 128–129, Feb., 2001.
[6] D. Draxelmayr, "A 6b 600MHz 10mW ADC Array in Digital 90nm CMOS," *Proc. of IEEE Solid-State Circ. Conf. (ISSCC)*, San Francisco, California, pp. 264–265, Feb., 2004.
[7] B. E. Jonsson, and R. Sundblad, "ADC's for sub-micron technologies," *EE Times Europe*, pp. 29–30, Apr. 21, 2008.
[8] A. M. A. Ali, C. Dillon, R. Sneed, A. S. Morgan, S. Bardsley, J. Kornblum, and L. Wu, "A 14-bit 125 MS/s IF/RF Sampling Pipelined ADC With 100 dB SFDR and 50 fs Jitter," *IEEE J. Solid-State Circuits*, Vol. 41, pp. 1846–1855, Aug, 2006.
[9] S. Rabii, and B. A. Wooley, "A 1.8-V digital-audio sigma-delta modulator in 0.8-µm CMOS," *IEEE J. Solid-State Circuits*, Vol. 32, pp. 783–795, June, 1997.
[10] R. Schreier and G. C. Temes, *Understanding Delta-Sigma Data Converters*, New York: Wiley-Interscience, 2005.
[11] T. N. Andersen, A. Briskemyr, F. Telstø, J. Bjørnsen, T. E. Bonerud, B. Hernes, and Ø. Moldsvor, "A 97mW 110MS/s 12b Pipeline ADC Implemented in 0.18µm Digital CMOS," *Proc. of Eur. Solid-State Circ. Conf. (ESSCIRC)*, Leuven, Belgium, pp. 247–250, Sept., 2004.
[12] B. Esperança, J. Goes, R. Tavares, A. Galhardo, N. Paulino, M. Medeiros Silva, "Power-and-area efficient 14-bit 1.5 MSample/s two-stage algorithmic ADC based on a mismatch-insensitive MDAC," *Proc. of ISCAS*, Seattle, Washington, USA, pp. 220–223, May, 2008.
[13] J. Sauerbrey, T. Tille, D. Schmitt-Landsiedel, and R. Thewes, "A 0.7-V MOSFET-only switched-opamp ∑Δ modulator in standard digital CMOS technology," *IEEE J. Solid-State Circuits*, Vol. 37, pp. 1662–1669, Dec., 2002.
[14] Y. Chiu, P. R. Gray, and B. Nikolic, "A 14-b 12-MS/s CMOS pipeline ADC with over 100-dB SFDR," *IEEE J. Solid-State Circuits*, Vol. 39, pp. 2139–2151, Dec., 2004.
[15] B. Bechen, T. v. d. Boom, D. Weiler, and B. J. Hosticka, "Theoretical and practical minimum of the power consumption of 3 ADCs in SC technique," *Proc. of Eur. Conf. Circ. Theory and Design (ECCTD)*, Seville, Spain, pp. 444–447, Aug., 2007.
[16] S. Gambini, and J. Rabaey, "A 1.5MS/s 6-bit ADC with 0.5V supply," *Proc. of IEEE Asian Solid-State Circ. Conf. (ASSCC)*, Hangzhou, China, pp. 47–50, Nov., 2006.
[17] W. C. Black, Jr., and D. A. Hodges, "Time interleaved converter arrays," *IEEE J. Solid-State Circuits*, Vol. SC-15, pp. 1022–1029, Dec., 1980.
[18] K. G. Merkel, and A. L. Wilson, "A survey of high performance analog-to-digital converters for defense space applications," in *Proc. IEEE Aerospace Conf.*, Big Sky, Montana, Mar. 2003, vol. 5, pp. 2415–2427.
[19] M. Vogels, and G. Gielen, "Architectural Selection of A/D Converters," *Proc. of Des. Aut. Conf. (DAC)*, Anaheim, California, USA, pp. 974–977, June, 2003.
[20] K. Bult, "Embedded analog-to-digital converters," *Proc. of Eur. Solid-State Circ. Conf. (ESSCIRC)*, Athens, Greece, pp. 52–60, Sept., 2009.
[21] B. E. Jonsson, "An empirical approach to finding energy efficient ADC architectures," Accepted for presentation at *IMEKO Int. Workshop ADC (IWADC)*, Orvieto, Italy, June, 2011.
[22] B. E. Jonsson, "On CMOS scaling and A/D-converter performance," *Proc. of NORCHIP*, Tampere, Finland, pp. 1–4, Nov. 2010.